IOPscience iopscience.iop.org

Home Search Collections Journals About Contact us My IOPscience

Rotational dephasing of a gold complex probed by anisotropic femtosecond x-ray solution scattering using an x-ray free-electron laser

This content has been downloaded from IOPscience. Please scroll down to see the full text.

2015 J. Phys. B: At. Mol. Opt. Phys. 48 244005

(http://iopscience.iop.org/0953-4075/48/24/244005)

View the table of contents for this issue, or go to the journal homepage for more

Download details:

IP Address: 143.248.94.107
This content was downloaded on 09/11/2015 at 01:32

Please note that terms and conditions apply.

IOP Publishing Journal of Physics B: Atomic, Molecular and Optical Physics
J. Phys. B: At. Mol. Opt. Phys. **48** (2015) 244005 (8pp) doi:10.1088/0953-4075/48/24/244005

Rotational dephasing of a gold complex probed by anisotropic femtosecond x-ray solution scattering using an x-ray free-electron laser

Jong Goo Kim[1,2], Kyung Hwan Kim[1,2], Key Young Oang[1,2], Tae Wu Kim[1,2], Hosung Ki[1,2], Junbeom Jo[1,2], Jeongho Kim[3], Tokushi Sato[4,5], Shunsuke Nozawa[4], Shin-ichi Adachi[4] and Hyotcherl Ihee[1,2]

[1] Department of Chemistry, KAIST, Daejeon 305-701, Korea
[2] Center for Nanomaterials and Chemical Reactions, Institute for Basic Science (IBS), Daejeon 305-701, Korea
[3] Department of Chemistry, Inha University, Incheon 402-751, Korea
[4] Institute of Materials Structure Science High Energy Accelerator Research Organization (KEK), 1-1 Oho, Tsukuba, Ibaraki 305-0801, Japan

E-mail: hyotcherl.ihee@kaist.ac.kr

Received 1 June 2015, revised 31 July 2015
Accepted for publication 16 September 2015
Published 3 November 2015

Abstract

The orientational dynamics of a gold trimer complex in a solution are investigated by using anisotropic femtosecond x-ray solution scattering measured by an x-ray free-electron laser. A linearly polarized laser pulse preferentially excites molecules with transition dipoles oriented parallel to the laser polarization, leading to the transient alignment of excited molecules. Such photoselectively aligned molecules give rise to an anisotropic scattering pattern that has different profiles in parallel and perpendicular directions with respect to laser polarization. Anisotropic x-ray scattering patterns obtained from the transiently aligned molecules contain information on the molecular orientation. By monitoring the time evolution of the anisotropic scattering pattern, we probe the rotational dephasing dynamics of $[Au(CN)_2^-]_3$ in a solution. We found that rotational dephasing of $[Au(CN)_2^-]_3$ occurs with a time constant of 13 ± 4 ps. By contrast, time-resolved scattering data on $FeCl_3$ in a water solution, which does not accompany any structural change and gives only the contributions of solvent heating, lacks any anisotropy in the scattering signal.

Keywords: anisotropic x-ray solution scattering, rotational dephasing, XFEL

(Some figures may appear in colour only in the online journal)

1. Introduction

Time-resolved x-ray solution scattering (TRXSS)—also known as time-resolved x-ray liquidography (TRXL)—is a useful tool for investigating molecular structural dynamics with a high spatiotemporal resolution. TRXSS makes use of a pump-probe scheme that employs a pump laser pulse for initiating a chemical reaction and a probe x-ray pulse for probing the photo-induced structural changes of reacting molecules. TRXSS has been applied to the photoreactions of various molecular systems in a solution, ranging from small molecules [1–14] to proteins [15–26], and has elucidated their detailed structural dynamics. In principle, an x-ray solution scattering pattern contains direct information on three-dimensional molecular structures, but the information on

[5] *Present address*: Center for Free-Electron Laser Science, Deutsches Elektronen-Synchrotron, Notkestrasse 85, 22607 Hamburg, Germany.

 © 2015 IOP Publishing Ltd Printed in the UK

molecular orientation is averaged out due to the random orientation of molecules in a solution. For this reason, previous TRXSS studies have mainly focused on the dynamics of intramolecular structural rearrangement rather than the orientational dynamics of molecules. Recently, it was suggested that anisotropic scattering patterns obtained by using linearly polarized laser light could be used to probe molecular orientation. For example, anisotropic patterns measured for myoglobin in a solution were analyzed to extract the dynamics of molecular orientation of the protein at the picosecond time scale [19]. In that work, linearly polarized laser pulses were used to create the excited protein molecules that are transiently aligned along the laser polarization direction. The photoselectively aligned molecules yielded anisotropic x-ray scattering patterns that have different scattering profiles in the vertical and horizontal regions of a scattering image. The discrepancy between the scattering profiles in the vertical and horizontal regions was monitored as a function of time, revealing the rotational dephasing time of the excited protein molecules in a solution.

This approach is similar to pump-probe transient anisotropy measured by time-resolved spectroscopy. Transient anisotropy can provide the orientational dynamics of molecules in isotropic media [27–29] and has been applied to the investigation of the rotational dephasing of molecules [30, 31] and energy transfer dynamics in multichromophore systems [32–36]. In the pump-probe transient anisotropy experiment, a linearly polarized pump laser pulse induces a transient anisotropic orientational distribution of excited molecules with their transition dipoles to be preferentially aligned along a laser polarization direction. Then, the evolution of a transient dipole direction is monitored by another linearly polarized probe pulse.

Even though previous anisotropic picosecond x-ray solution scattering performed on myoglobin has demonstrated that TRXSS can be applied to the study of molecular orientational dynamics, the technique could not be applied to small molecules. This is because the time resolution of the TRXSS experiment using a synchrotron is only $\sim$100 ps and is not fast enough to observe their orientational dynamics. With the advent of x-ray free-electron lasers (XFELs) that generate sub-100 fs x-ray pulses, anisotropic x-ray solution scattering can be extended to the orientational dynamics of small molecules.

In this work, we present the first example in which the orientational dynamics of a small molecule in the solution phase have been revealed by TRXSS. We performed a TRXSS experiment on a gold trimer complex, $[Au(CN)_2^-]_3$, in an aqueous solution and monitored the transient anisotropy using anisotropic scattering patterns to elucidate its orientational dynamics.

2. Experimental

The experimental setup of TRXSS and the geometry of the laser and x-ray beams are schematically shown in figure 1(a). A laser pulse initiates a photoreaction of sample molecules in the solution phase. In particular, the linearly polarized laser pulse induces the photoselective alignment of the excited molecules. Subsequently, a femtosecond x-ray pulse generated by an XFEL is scattered from the sample molecules, yielding an anisotropic scattering pattern. The x-ray pulse incident with a time delay, Δt, with respect to the laser pulse, monitors the time evolution of the anisotropy in the scattering patterns as well as the progress of the reaction.

In our experiment, the x-ray beam propagated along the z-axis and the sample was flown along the x-axis in a laboratory-fixed reference frame. The laser beam was overlapped with the x-ray beam at the focal point at a crossing angle of 10°, resulting in a laser polarization direction, ε, parallel to the ground and tilted by 10° with respect to the y-axis as shown in figure 1(a). When a linearly polarized laser pulse interacts with an ensemble of molecules, the excitation probability of a molecule with a transition dipole, μ, is proportional to $\cos^2\alpha$, where α is the angle between the laser polarization (ε) and the transition dipole (μ). As a result, the orientational distribution of the excited molecules is transiently anisotropic at the moment of laser excitation.

In this work, we performed a femtosecond TRXSS experiment on $[Au(CN)_2^-]_3$ in a solution at the BL3 beamline of SACLA by using x-ray pulses with a sub-100 fs temporal width. The center energy of the x-rays was 15 keV with a narrow bandwidth ($\Delta E/E = 0.6\%$). The x-ray beam was focused on a spot 200 μm in diameter, yielding a fluence of 1.3 mJ mm^{-2}. The laser pulses of 100 fs in duration at a 267 nm wavelength were generated by the third-harmonic generation of femtosecond laser pulses at an 800 nm wavelength from a Ti:sapphire regenerative amplifier. The 267 nm laser pulses were focused on a spot 300 μm in diameter, yielding a fluence of 2.1 mJ mm^{-2}. The x-ray scattering patterns were collected using an area detector (Rayonix, LX255-HS) with a sample-to-detector distance of 31 mm. The $[Au(CN)_2^-]_3$ solution of 300 mM concentration was used to maximize the formation of the gold trimer complex against the formation of monomeric and dimeric complexes. For comparison, we measured the TRXSS signals of $FeCl_3$ in water (40 mM concentration), which gives only the contributions of solvent heating. The sample solutions were circulated using a sapphire nozzle with a 100 μm thick aperture. The sample was made to flow with a flow speed higher than 3 m s^{-1} to supply fresh samples for every pair of laser and x-ray pulses. To obtain time-resolved difference scattering intensities, 'laser-off' images measured at a reference time delay (that is, a –200 ps time delay) were subtracted from 'laser-on' images collected at time delays from –800 fs to 100 ps. Scattering intensities arising from 80 x-ray pulses were accumulated for each scattering image to minimize the x-ray intensity fluctuation caused by the SASE process. At each time delay, about 50 images were collected to achieve a high signal-to-noise ratio.

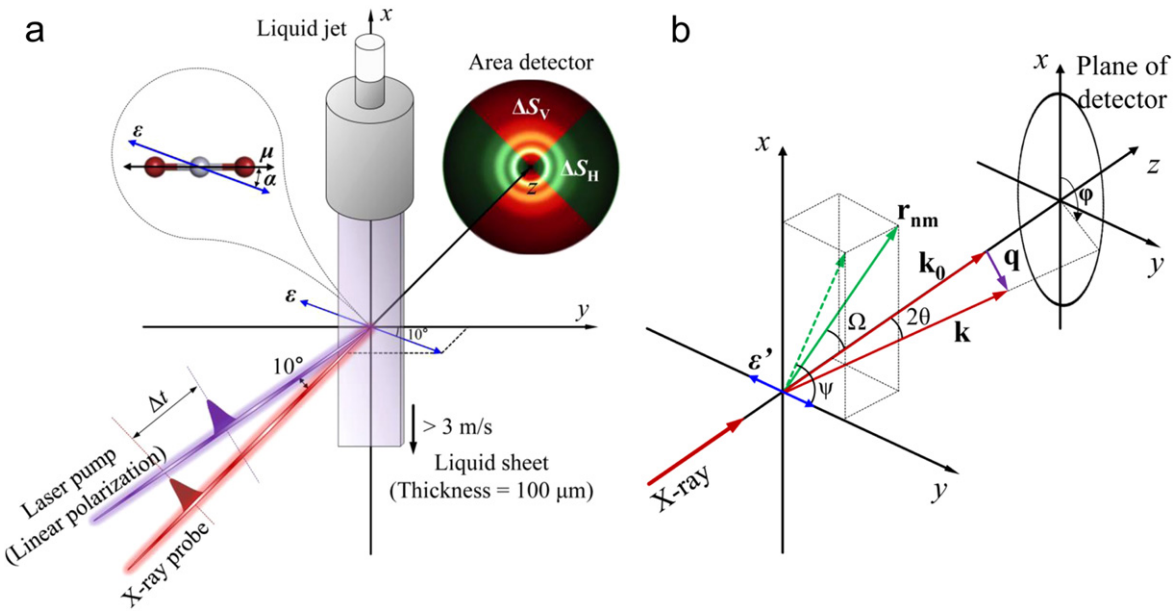

Figure 1 (a) Schematic of TRXSS experiment and the experimental geometry represented in a laboratory-fixed reference frame. Sample molecules in a solution are excited by a linearly polarized laser pulse, resulting in the excited molecules transiently aligning along the laser polarization direction. Subsequently, a femtosecond x-ray pulse incident with a time delay, Δt, probes the changes in molecular orientation as well as the molecular structure with the progress of the photoinduced reaction. In our experiment, the x-ray beam propagated along the x-axis and the sample was flown along the z-axis. The laser beam was overlapped with the x-ray beam at the focal point at a crossing angle of 10°, resulting in a laser polarization direction, ε, parallel to the ground and tilted by 10° with respect to the y-axis. The transient aligned molecules generate an anisotropic scattering pattern. To examine the anisotropy in the scattering image, we performed azimuthal integrations for vertical and horizontal regions separately, yielding two distinct difference scattering curves, $\Delta S_V(q, t)$ and $\Delta S_H(q, t)$, respectively. (b) Geometry of x-ray scattering experiment defined for the theoretical description of anisotropic x-ray scattering patterns. The position vector between the nth and mth atoms (green arrow), $\mathbf{r_{nm}}$, is defined by the spherical-coordinate variables, Ω and ψ, where Ω is the altitude angle relative to the z-axis and ψ is the azimuthal angle relative to the y-axis. The momentum transfer vector (purple arrow), $\mathbf{q}$, represents the momentum transfer between the incident ($\mathbf{k_0}$) and the scattered ($\mathbf{k}$) x-ray waves, and its magnitude is dependent on the scattering angle, 2θ, and the azimuthal angle, φ, of the scattered x-ray beam. The direction of laser polarization (blue arrow), ε', was considered to be parallel to the y-axis.

3. Theoretical description of anisotropic x-ray scattering pattern

Theoretical models for anisotropic scattering patterns arising from an ensemble of unidirectionally oriented molecules have previously been developed [19, 37–41]. Here, we briefly present a theoretical description of anisotropic x-ray scattering patterns based on the derivation by Williamson *et al* [41]. Although this formalism was originally derived for electron diffraction, it is still valid for x-ray scattering within the independent atom model. The x-ray scattering intensity, $S(q)$, of molecules in a solution can be expressed as

$$S(\mathbf{q}) = \sum_n \sum_m f_n(q) f_m(q) \left\langle \exp\left(-i\mathbf{q}\cdot\mathbf{r}_{nm}\right)\right\rangle_{orientation} \quad (1)$$

where the indexes m and n refer to all atoms in the solution sample, and $\mathbf{q}$ is the momentum transfer vector between the incident ($\mathbf{k_0}$) and the scattered ($\mathbf{k}$) x-ray waves with its magnitude given by $q = 4\pi/\lambda \cdot \sin(2\theta/2)$, where 2θ is the scattering angle and λ is the x-ray wavelength. $\mathbf{r}_{nm}$ denotes the position vector between the nth and mth atoms, and $f_n(q)$ and $f_m(q)$ are the x-ray atomic form factors of the nth and mth atoms, respectively. We consider only the elastic x-ray scattering intensity because inelastic x-ray scattering does not affect the difference x-ray scattering intensity. The symbol $\langle\rangle_{orientation}$ represents the rotational average over all the possible molecular orientations defined by the spherical-coordinate variables (Ω and ψ), where Ω is the altitude angle relative to the z-axis and ψ is the azimuthal angle relative to the y-axis as shown in figure 1(b).

The scattering intensity in equation (1) is generally used for isotropically oriented molecules but can be extended to anisotropically oriented molecules by introducing an appropriate orientational distribution function, $P(\Omega, \psi)$, as follows:

$$\begin{aligned} S(\mathbf{q}) &= \sum_n \sum_m f_n(q) f_m(q) \\ &\quad \times \left\langle P(\Omega,\psi)\exp\left(-i\mathbf{q}\cdot\mathbf{r}_{nm}\right)\right\rangle_{orientation} \\ &= \sum_n \sum_m f_n(q) f_m(q) \frac{1}{4\pi} \\ &\quad \times \int_0^{\pi}\int_0^{2\pi} P(\Omega,\psi)\exp\left(-i\mathbf{q}\cdot\mathbf{r}_{nm}\right)\sin\Omega d\psi d\Omega \end{aligned} \quad (2)$$

To evaluate $S(q)$, we used a geometrical reference frame shown in figure 1(b). In the reference frame, $\mathbf{q}$ and $\mathbf{r}_{nm}$ can be written as

$$\mathbf{q} = q(-\cos\varphi\cos\theta, -\sin\varphi\cos\theta, \sin\theta) \quad (3)$$

$$\mathbf{r}_{nm} = r_{nm}(\sin\Omega\sin\psi, \sin\Omega\cos\psi, \cos\Omega) \quad (4)$$

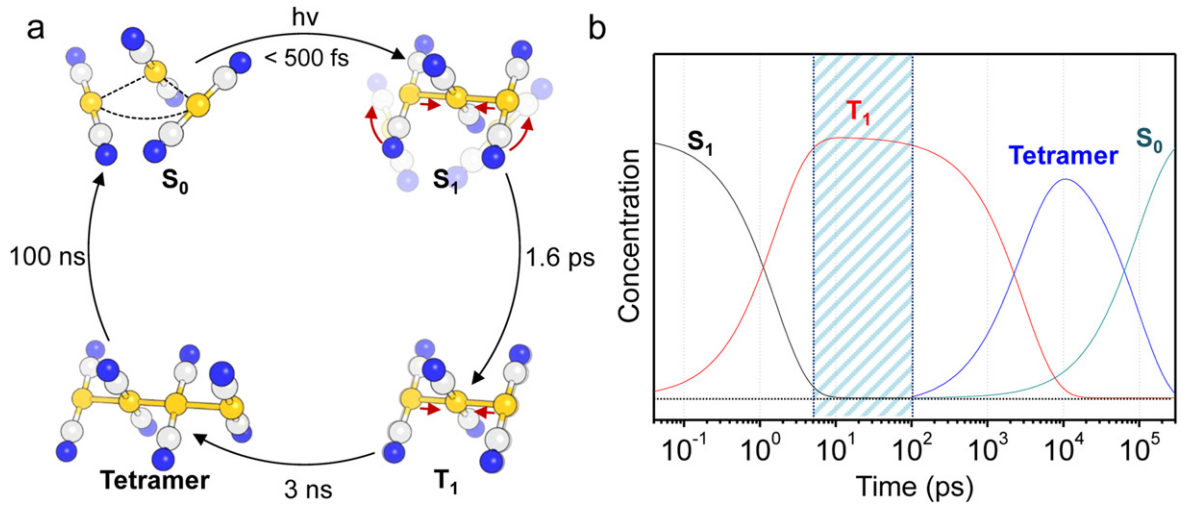

Figure 2. (a) Structural dynamics of $[Au(CN)_2^-]_3$ in an aqueous solution. In the ground S_0 state, the gold atoms are bound in close proximity by a non-covalent interaction called aurophilicity. Upon laser excitation, covalent bonds are formed between adjacent gold atoms with a bent-to-linear structural change within ~500 fs. The S_1 state is converted into T_1 with a time constant of 1.6 ps while accompanying further bond shortening. Then, a tetramer is formed with a time constant of 3 ns and finally returns back to S_0 with a time constant of 100 ns. (b) Concentration changes of the four states of $[Au(CN)_2^-]_3$ as a function of time. As shown in figure 4, the time evolution of the anisotropy was monitored in the time range from 5.2 ps to 105.2 ps (blue shaded area). Therefore, the orientational dynamics investigated in this work are characteristic of the T_1 state of $[Au(CN)_2^-]_3$.

where φ represents the azimuthal angle (relative to the x-axis) of the scattered x-ray beam as shown in figure 1(b). To simplify the evaluation of equation (2), we will only consider scattering from atomic pairs that have $\mathbf{r}_{nm}$ parallel to the direction of the transition dipole of each molecule.

For isotropically oriented molecules, the distribution function is given by $P(\Omega, \psi) = 1$. By inserting equations (3) and (4) into equation (2), we obtain the well-known Debye equation as follows:

$$S(\mathbf{q}) = \sum_n \sum_m f_n(q) f_m(q) j_0(qr_{nm}) = \sum_n \sum_m f_n(q) f_m(q) \frac{\sin(qr_{nm})}{qr_{nm}} \quad (5)$$

where j_0 is the first spherical Bessel function and r_{nm} denotes the magnitude of $\mathbf{r}_{nm}$. It can be seen that the azimuthal angle, φ, is absent in equation (5), indicating that the scattering pattern arising from isotropically orientated molecules is isotropic (or centrosymmetric).

For anisotropically oriented molecules, here we consider a simple case where the direction of laser polarization (ε') is parallel to the y-axis as shown in figure 1(b). In this case, the distribution function is given by $P(\Omega, \psi) = \sin^2\Omega \cos^2\psi$. Then, $S(q)$ is expressed by

$$S(\mathbf{q}) = \sum_n \sum_m f_n(q) f_m(q) \times \left(\frac{j_1(qr_{nm})}{qr_{nm}} + \cos^2\theta j_2(qr_{nm}) \cos^2\varphi \right) \quad (6)$$

where j_1 and j_2 are the second and third spherical Bessel functions, respectively. Equation (6) clearly shows that the x-ray scattering intensity depends on the azimuthal angle, φ, and therefore the scattering patterns arising from an anisotropic orientational distribution of molecules should be anisotropic. As a result, the degree of anisotropy of an x-ray scattering pattern can serve as a measure of the orientational distribution of target molecules. In addition, the temporal change of the anisotropy in a series of time-resolved x-ray scattering patterns directly reflects the dynamics of anisotropic-to-isotropic orientational redistribution.

4. Structural dynamics of $[Au(CN)_2^-]_3$ in a solution

A chemical reaction occurs by the formation and breaking of chemical bonds and therefore a complete understanding of chemical reactions essentially requires the monitoring of such bond making and breaking processes. Ultrafast bond-breaking processes have been intensively studied by using time-resolved techniques. However, bond-making processes have been studied much less frequently because they are diffusion-limited bimolecular processes and are thus hard to initiate by laser excitation. A gold trimer complex, $[Au(CN)_2^-]_3$, is a good molecular system for investigating bond formation because a non-covalent interaction among gold atoms (called aurophilicity) allows the atoms constituting the complex to reside in the same solvent cage. As a result, bond formation in a gold trimer complex can be triggered by a laser pulse without being limited by diffusion. We recently performed TRXSS on a gold trimer complex and have revealed the structural dynamics involving bond formation between gold atoms, bent-to-linear structural relaxation, and tetramer formation [1]. We have summarized the dynamics of the gold trimer complex in figure 2(a). By the kinetic and structural analysis of the TRXSS data measured for $[Au(CN)_2^-]_3$, we identified four structurally distinct states: the ground state (S_0), an excited state (S_1), a triplet state (T_1), and a tetramer.

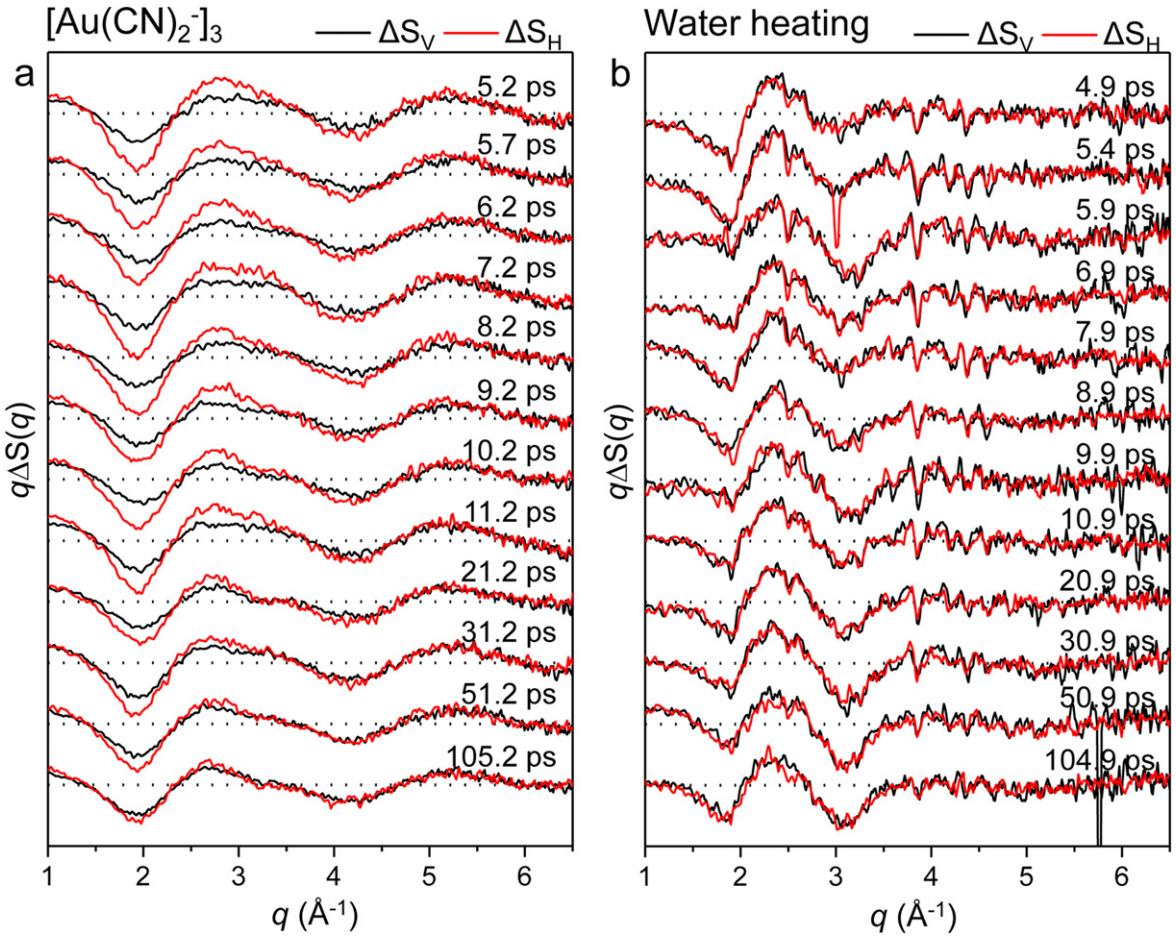

Figure 3. (a) Experimental difference scattering curves of $[Au(CN)_2^-]_3$ in a solution measured at time delays from 5.2 ps to 105.2 ps. Difference scattering curves, ΔS_V (black lines) and ΔS_H (red lines), were obtained by the azimuthal integration of the vertical and horizontal region of the 2D scattering images, respectively. (b) Experimental difference scattering curves of solvent heating induced by the excitation of $FeCl_3$ in an aqueous solution measured at time delays from 4.9 ps to 104.9 ps. ΔS_V and ΔS_H are shown with black and red curves, respectively.

Upon laser excitation, an electron in S_0 is excited from an antibonding to a bonding orbital. As a result, covalent bonds are formed between adjacent gold atoms in the S_1 state. We found that by the transition from S_0 to S_1, the average distance between adjacent gold atoms decreases from 3.6 Å to 2.8 Å by the formation of covalent bonds. Furthermore, the structural change from bent to linear geometry occurs within ~500 fs, which is the experimental time resolution. Subsequently, the S_1 state is converted into T_1 with a time constant of 1.6 ps while accompanying further bond shortening. Then, a tetramer is formed with a time constant of 3 ns and finally returns back to S_0 with a time constant of 100 ns.

In this work, rather than bond formation dynamics, we focus on the orientational dynamics of the gold trimer complex by analyzing the anisotropic patterns of the TRXSS data in the time range from 5.2 ps to 100 ps, where no distinct kinetic component is present due to structural transitions according to our prior study [1]. In figure 2(b), the concentration changes of the four states are shown and the time window used for studying the orientational dynamics is indicated by a blue shaded area. The orientational dynamics of the T_1 state of $[Au(CN)_2^-]_3$ will be specifically discussed below.

5. Orientational dynamics of $[Au(CN)_2^-]_3$ extracted from anisotropic scattering patterns

In a TRXSS experiment, a 2D scattering image arising from a reaction intermediate in a solution is recorded using an area detector. When the transient intermediate molecules are randomly oriented in a solution, the scattering image is centrosymmetric as described in section 3. In this case, a 1D scattering curve is obtained by azimuthally integrating the 2D image as a function of the momentum transfer vector, **q**, and the 1D scattering curve contains the same structural information as the original 2D scattering image. In contrast, when the excited molecules are aligned photoselectively, an anisotropic 2D scattering image is obtained. If the anisotropic 2D scattering image is azimuthally integrated into a 1D scattering curve, the information on the anisotropy of the 2D scattering image will be obscured. Instead, to properly extract the anisotropic information, azimuthal integration only needs to be

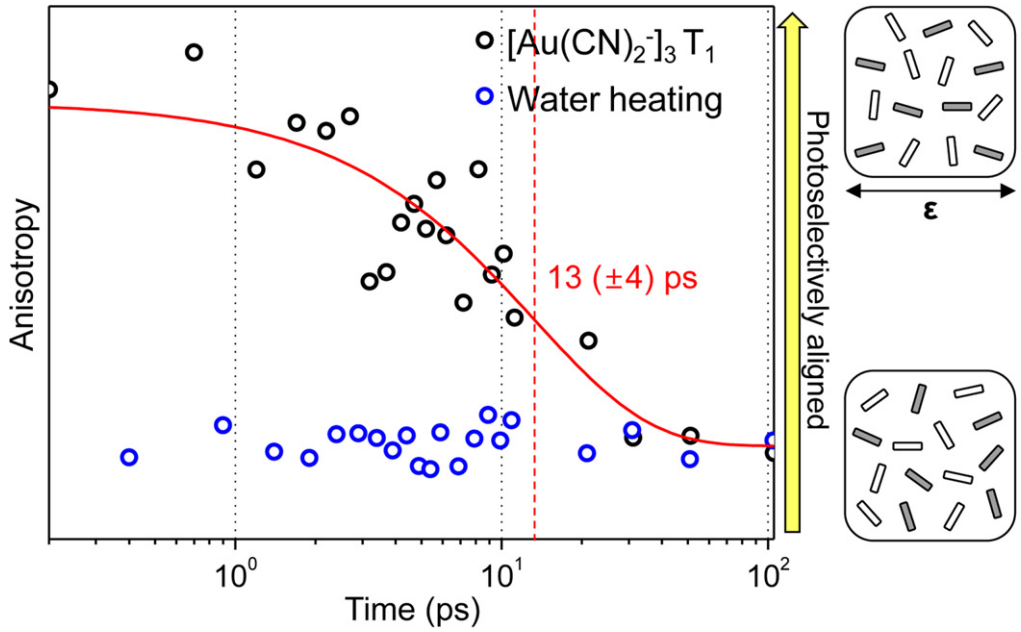

Figure 4. Transient anisotropy of $[Au(CN)_2^-]_3$ (black circles) and solvent heating (blue circles) extracted from the TRXSS measurement. A high anisotropy value is obtained when the discrepancy between ΔS_H and ΔS_V is large. The transient anisotropy of $[Au(CN)_2^-]_3$ decays over time and can be fit with a single exponential with a time constant of 13 ± 4 ps. In contrast, the transient anisotropy arising from solvent heating is small and stays constant over time.

performed for the truncated regions. To do so, we dissected the scattering image into vertical and horizontal regions, as shown in figure 1(a), and obtained two distinctly different scattering curves, $\Delta S_V(q, t)$ and $\Delta S_H(q, t)$, by azimuthally integrating the vertical and horizontal regions, respectively. Specifically, $\Delta S_V(q, t)$ and $\Delta S_H(q, t)$ were obtained as follows:

$$\Delta S_V(q, t) = \int_{-\pi/4}^{\pi/4} \Delta S(\mathbf{q}, t) d\varphi + \int_{3\pi/4}^{5\pi/4} \Delta S(\mathbf{q}, t) d\varphi \quad (7)$$

$$\Delta S_H(q, t) = \int_{\pi/4}^{3\pi/4} \Delta S(\mathbf{q}, t) d\varphi + \int_{5\pi/4}^{7\pi/4} \Delta S(\mathbf{q}, t) d\varphi \quad (8)$$

As can be expected from equation (6), anisotropically oriented molecules will yield $\Delta S_V(q, t)$ and $\Delta S_H(q, t)$ distinct from each other. The discrepancy between $\Delta S_V(q, t)$ and $\Delta S_H(q, t)$ represents the degree of anisotropy of the scattering image, which is directly related to the orientational distribution of the molecules. Thus, the decay of the discrepancy between $\Delta S_V(q, t)$ and $\Delta S_H(q, t)$ indicates that the orientational distribution of the excited molecules changes from an anisotropic distribution to an isotropic one, that is to say, rotational dephasing.

In figure 3(a), $\Delta S_V(q, t)$ and $\Delta S_H(q, t)$ for the T_1 state of $[Au(CN)_2^-]_3$ are shown. The oscillatory features in ΔS_V and ΔS_H at a 5.2 ps time delay clearly have different amplitudes from each other. As the time delay increases, the difference between the two curves becomes smaller and ΔS_V and ΔS_H are identical at 105.2 ps. This observation suggests that the transition dipole of the T_1 state is aligned preferentially along the laser polarization direction at a 5.2 ps time delay but the orientation of the transition dipole becomes randomized over time through rotational dephasing. For comparison, we performed a separate TRXSS experiment on $FeCl_3$ in a solution. When $FeCl_3$ is illuminated by a laser pulse at 267 nm, the excited $FeCl_3$ molecules do not undergo any structural change, such as bond formation or breaking. Instead, the excitation energy absorbed by the $FeCl_3$ molecules is thermally dissipated into the surrounding solvent molecules, resulting in a temperature increase of the solvent at early time delays and a density decrease of the solvent at late time delays. Such collective structural changes in solvent molecules give rise to distinct difference scattering signals of solvent heating [42]. If the solute-to-solvent heat transfer and the subsequent solvent-to-solvent heat transfer occur anisotropically, the collective structural change in solvent molecules should occur favorably in a certain direction, thus yielding an anisotropic scattering pattern. We examined whether the scattering images arising from solvent heating contain any anisotropy. As can be seen in figure 3(b), $\Delta S_V(q, t)$ and $\Delta S_H(q, t)$ of the scattering signal arising from solvent heating are identical to each other in the entire time range of the TRXSS measurement. The lack of anisotropy in the scattering patterns of solvent heating indicates that solute-to-solvent heat transfer does not induce any observable anisotropic distribution of the heated solvent molecules within the available time resolution.

To quantify the degree of anisotropy reflected in the scattering images of $[Au(CN)_2^-]_3$, we calculated the transient anisotropy, $r(t)$, for the scattering image at each time delay as

follows:

$$r(t) = \left(\left(\sum_i \left| \left(\Delta S_H(q_i, t) - \Delta S_V(q_i, t) \right) / \sqrt{\sigma_H^2(q_i, t) + \sigma_V^2(q_i, t)} \right| \right) / \left(\sum_i \left| \Delta S_H(q_i, t) \right| + \sum_i \left| \Delta S_V(q_i, t) \right| \right) \right) \quad (9)$$

where $\sigma_H(q_i, t)$ and $\sigma_V(q_i, t)$ are the standard deviations of $\Delta S_H(q_i, t)$ and $\Delta S_V(q_i, t)$, respectively, at each q-point determined from 50 independent measurements. To consider the experimental noise at each q-point, the difference between $\Delta S_H(q, t)$ and $\Delta S_H(q, t)$ at each q-point was divided by the corresponding standard deviation, $\sqrt{\sigma_H^2(q_i, t) + \sigma_V^2(q_i, t)}$, as can be seen in equation (9). The summation (or integration) in the q-domain was performed in the q-range from 1.0 Å^{-1} to 6.5 Å^{-1}. To account for the time-dependent amplitude change of the time-resolved difference scattering signal, we normalized the transient anisotropy by further dividing the difference between $\Delta S_H(q, t)$ and $\Delta S_H(q, t)$ by the total area under the $\Delta S_H(q, t)$ and $\Delta S_H(q, t)$ curves, $\sum_i \left| \Delta S_H(q_i, t) \right| + \sum_i \left| \Delta S_V(q_i, t) \right|$, at each time point. The calculated $r(t)$ represents the degree of anisotropy in the transient orientational distribution of the excited molecules in a solution. As the discrepancy between $\Delta S_H(q, t)$ and $\Delta S_V(q, t)$ becomes larger, a higher $r(t)$ value is obtained, as expected from equation (9).

The time profiles of $r(t)$ for $[Au(CN)_2^-]_3$ and $FeCl_3$ in the time range from 5.2 ps to 105.2 ps are shown in figure 4. It can clearly be seen that the $r(t)$ of $[Au(CN)_2^-]_3$ decays over time. In contrast, the $r(t)$ of $FeCl_3$ stays constant, as was expected from the lack of anisotropy in figure 3(b). Because the T_1 state is the only dominant species in the time range of 5.2–100 ps as shown in figure 2(b), the decay of $r(t)$ must represent the orientational dynamics of the T_1 state. The observed $r(t)$ decay of $[Au(CN)_2^-]_3$ can be fit with a single exponential with a time constant of 13 (±4) ps, which corresponds to the rotational dephasing time of $[Au(CN)_2^-]_3$. The rotational dephasing time of $[Au(CN)_2^-]_3$ is in good agreement with the theoretical value (~10 ps) predicted using the Stokes–Einstein equation for a sphere with the same volume as a $[Au(CN)_2^-]_3$ molecule. The slightly slower orientational dynamics obtained from the experiment may result from the nonspherical shape of $[Au(CN)_2^-]_3$, which will experience a larger frictional force than the sphere.

6. Conclusion

The rotational dephasing of a gold trimer complex, $[Au(CN)_2^-]_3$ was investigated by femtosecond anisotropic x-ray solution scattering using ultrashort x-ray pulses generated by an XFEL. The anisotropic scattering patterns provide information on molecular orientation and thus increase the information content of TRXSS data beyond the intramolecular structure. Consideration of anisotropy in scattering patterns has now become more important with the advent of XFEL because they are necessarily observed on time scales from femtoseconds to picoseconds. Our present work offers a strategy for the data analysis of anisotropic scattering patterns measured in femtosecond x-ray scattering experiments.

Acknowledgments

This work was supported by IBS-R004-G2 and the X-ray Free Electron Laser Priority Strategic Program of MEXT, Japan. This work was also supported by the Basic Science Research Program through the National Research Foundation of Korea (NRF) funded by the Ministry of Science, ICT & Future Planning (NRF-2014R1A1A1002511). The experiments were performed at the BL3 of SACLA with the approval of the Japan Synchrotron Radiation Research Institute (JASRI) (Proposal No. 2012A8030, 2012A8038, 2012B8029, 2012B8043, 2013A8053, 2013B8036, 2013B8059, 2014A8042 and 2014A8022).

References

[1] Kim K H *et al* 2015 Direct observation of bond formation in solution with femtosecond x-ray scattering *Nature* **518** 385–9
[2] Ihee H 2009 Visualizing solution-phase reaction dynamics with time-resolved x-ray liquidography *Acc. Chem. Res.* **42** 356–66
[3] Ihee H, Lorenc M, Kim T K, Kong Q Y, Cammarata M, Lee J H, Bratos S and Wulff M 2005 Ultrafast x-ray diffraction of transient molecular structures in solution *Science* **309** 1223–7
[4] Kim T K, Lee J H, Wulff M, Kong Q and Ihee H 2009 Spatiotemporal kinetics in solution studied by time-resolved x-ray liquidography (solution scattering) *Chem. Phys. Chem* **10** 1958–80
[5] Kim T K *et al* 2006 Spatiotemporal reaction kinetics of an ultrafast photoreaction pathway visualized by time-resolved liquid x-ray diffraction *Proc. Natl Acad. Sci. USA* **103** 9410–5
[6] Lee J H, Kim J, Cammarata M, Kong Q, Kim K H, Choi J, Kim T K, Wulff M and Ihee H 2008 Transient x-ray diffraction reveals global and major reaction pathways for the photolysis of iodoform in solution *Angew. Chem. Int. Ed.* **47** 1047–50
[7] Lee J H, Kim T K, Kim J, Kong Q, Cammarata M, Lorenc M, Wulff M and Ihee H 2008 Capturing transient structures in the elimination reaction of haloalkane in solution by transient x-ray diffraction *J. Am. Chem. Soc.* **130** 5834–5
[8] Vincent J, Andersson M, Eklund M, Wohri A B, Odelius M, Malmerberg E, Kong Q, Wulff M, Neutze R and Davidsson J 2009 Solvent dependent structural perturbations of chemical reaction intermediates visualized by time-resolved x-ray diffraction *J. Chem. Phys.* **130** 154502
[9] Plech A, Wulff M, Bratos S, Mirloup F, Vuilleumier R, Schotte F and Anfinrud P A 2004 Visualizing chemical reactions in solution by picosecond x-ray diffraction *Phys. Rev. Lett.* **92** 125505
[10] Canton S E *et al* 2015 Visualizing the non-equilibrium dynamics of photoinduced intramolecular electron transfer with femtosecond x-ray pulses *Nat. Commun.* **6** 6359

[11] Haldrup K *et al* 2011 Bond shortening (1.4 A) in the singlet and triplet excited states of [Ir2(dimen)4]2+ in solution determined by time-resolved x-ray scattering *Inorg. Chem.* **50** 9329–36
[12] Georgiou P, Vincent J, Andersson M, Wohri A B, Gourdon P, Poulsen J, Davidsson J and Neutze R 2006 Picosecond calorimetry: time-resolved x-ray diffraction studies of liquid CH2Cl2 *J. Chem. Phys.* **124** 234507
[13] Christensen M, Haldrup K, Bechgaard K, Feidenhans'l R, Kong Q Y, Cammarata M, Lo Russo M, Wulff M, Harrit N and Nielsen M M 2009 Time-Resolved x-ray scattering of an electronically excited state in solution. structure of the (3)A(2u) state of tetrakis-mu-pyrophosphitodiplatinate(II) *J. Am. Chem. Soc.* **131** 502–8
[14] Kim J, Kim K H, Lee J H and Ihee H 2010 Ultrafast x-ray diffraction in liquid, solution and gas: present status and future prospects *Acta Crystallogr., Sect.* A **66** 270–80
[15] Kim K H *et al* 2012 Direct observation of cooperative protein structural dynamics of homodimeric hemoglobin from 100 ps to 10 ms with pump-probe x-ray solution scattering *J. Am. Chem. Soc.* **134** 7001–8
[16] Kim T W *et al* 2012 Protein structural dynamics of photoactive yellow protein in solution revealed by pump-probe x-ray solution scattering *J. Am. Chem. Soc.* **134** 3145–53
[17] Cammarata M, Levantino M, Schotte F, Anfinrud P A, Ewald F, Choi J, Cupane A, Wulff M and Ihee H 2008 Tracking the structural dynamics of proteins in solution using time-resolved wide-angle x-ray scattering *Nat. Methods* **5** 881–6
[18] Kim K H, Oang K Y, Kim J, Lee J H, Kim Y and Ihee H 2011 Direct observation of myoglobin structural dynamics from 100 picoseconds to 1 microsecond with picosecond x-ray solution scattering *Chem. Commun.* **47** 289–91
[19] Kim J, Kim K H, Kim J G, Kim T W, Kim Y and Ihee H 2011 Anisotropic picosecond x-ray solution scattering from photo-selectively aligned protein molecules *J. Phys. Chem. Lett.* **2** 350–6
[20] Oang K Y, Kim J G, Yang C, Kim T W, Kim Y, Kim K H, Kim J and Ihee H 2014 Conformational substates of myoglobin intermediate resolved by picosecond x-ray solution scattering *J. Phys. Chem. Lett.* **5** 804–8
[21] Oang K Y, Kim K H, Jo J, Kim Y, Kim J G, Kim T W, Jun S, Kim J and Ihee H 2014 Sub-100-ps structural dynamics of horse heart myoglobin probed by time-resolved x-ray solution scattering *Chem. Phys.* **422** 137–42
[22] Arnlund D *et al* 2014 Visualizing a protein quake with time-resolved x-ray scattering at a free-electron laser *Nat. Methods* **11** 923–6
[23] Malmerberg E *et al* 2011 Time-resolved WAXS reveals accelerated conformational changes in iodoretinal-substituted proteorhodopsin *Biophys. J.* **101** 1345–53
[24] Konuma T, Kimura T, Matsumoto S, Goto Y, Fujisawa T, Fersht A R and Takahashi S 2011 Time-resolved small-angle x-ray scattering study of the folding dynamics of barnase *J. Mol. Biol.* **405** 1284–94
[25] Ahn S, Kim K H, Kim Y, Kim J and Ihee H 2009 Protein tertiary structural changes visualized by time-resolved x-ray solution scattering *J. Phys. Chem.* B **113** 13131–3
[26] Cho H S, Dashdorj N, Schotte F, Graber T, Henning R and Anfinrud P 2010 Protein structural dynamics in solution unveiled via 100-ps time-resolved x-ray scattering *Proc. Natl Acad. Sci. USA* **107** 7281–6
[27] Szabo A 1984 Theory of fluorescence depolarization in macromolecules and membranes *J. Chem. Phys.* **81** 150–67
[28] Fourkas J T, Trebino R and Fayer M D 1992 The grating decomposition method—a new approach for understanding polarization-selective transient grating experiments: 1. Theory *J. Chem. Phys.* **97** 69–77
[29] Tokmakoff A 1996 Orientational correlation functions and polarization selectivity for nonlinear spectroscopy of isotropic media: 1. Third order *J. Chem. Phys.* **105** 1–12
[30] Baskin J S and Zewail A H 1994 Femtosecond real-time probing of reactions: 15. Time-dependent coherent alignment *J. Phys. Chem.* **98** 3337–51
[31] Brown E J, Pastirk I and Dantus M 1999 Ultrafast rotational anisotropy measurements: unidirectional detection *J. Phys. Chem.* A **103** 2912–6
[32] Kim Y R, Lee M, Thorne J R G, Hochstrasser R M and Zeigler J M 1988 Picosecond reorientations of the transition dipoles in polysilanes using fluorescence anisotropy *Chem. Phys. Lett.* **145** 75–80
[33] Kim J, Park S and Scherer N F 2008 Ultrafast dynamics of polarons in conductive polyaniline: comparison of primary and secondary doped forms *J. Phys. Chem.* B **112** 15576–87
[34] Jonas D M, Lang M J, Nagasawa Y, Joo T and Fleming G R 1996 Pump-probe polarization anisotropy study of femtosecond energy transfer within the photosynthetic reaction center of Rhodobacter sphaeroides R26 *J. Phys. Chem.* **100** 12660–73
[35] Mirkovic T, Doust A B, Kim J, Wilk K E, Curutchet C, Mennucci B, Cammi R, Curmi P M G and Scholes G D 2007 Ultrafast light harvesting dynamics in the cryptophyte phycocyanin 645 *Photochem. Photobiol. Sci.* **6** 964–75
[36] Jun S, Kim T W, Yang C, Isaji M, Tamiaki H, Ihee H and Kim J 2014 Ultrafast energy transfer in chlorosome probed by femtosecond pump-probe polarization anisotropy *Bull. Korean Chem. Soc.* **35** 703–4
[37] Ho P J, Starodub D, Saldin D K, Shneerson V L, Ourmazd A and Santra R 2009 Molecular structure determination from x-ray scattering patterns of laser-aligned symmetric-top molecules *J. Chem. Phys.* **131** 131101
[38] Lorenz U, Moller K B and Henriksen N E 2010 On the interpretation of time-resolved anisotropic diffraction patterns *New J. Phys.* **12** 113022
[39] Debnarova A, Techert S and Schmatz S 2011 Computational studies of the x-ray scattering properties of laser aligned stilbene *J. Chem. Phys.* **134** 054302
[40] Penfold T J, Tavernelli I, Abela R, Chergui M and Rothlisberger U 2012 Ultrafast anisotropic x-ray scattering in the condensed phase *New J. Phys.* **14** 113002
[41] Williamson J C and Zewail A H 1994 Ultrafast electron-diffraction: 4. Molecular-structures and coherent dynamics *J. Phys. Chem.* **98** 2766–81
[42] Cammarata M *et al* 2006 Impulsive solvent heating probed by picosecond x-ray diffraction *J. Chem. Phys.* **124** 124504